

INFLUENCE OF THE MINING SUBSOIL DEFORMATION ON THE VALUES OF FORCES IN REINFORCEMENT OF REINFORCED RETAINING WALL

JAN GASZYŃSKI, MARIUSZ POSLAJKO

Cracow University of Technology, Department of Environmental Engineering,
Institute of Geotechnics, 24 Warszawska St., 31-155 Cracow, Poland.
Phone: 0048-12-628-28-20. Fax: 0048-12-628-28-66. E-mail: jgaszyn@usk.pk.edu.pl

Abstract: An example of numerical 2D analysis of reinforced retaining wall subjected to mining subsoil deformation is presented. This subsoil strain has been described by the parameters of subsoil mining subsidence. In numerical analysis, the influence of mining subsidence has been transferred to the structure by an area of soil. An elastic-plastic Drucker–Prager model and Cap model in plain strain for subsoil and embankment have been used in the FEM.

1. INTRODUCTION

In the engineering practice, reinforced retaining walls are very often formed. In comparison with the reinforced concrete walls, they make the forming easier and allow us to reduce costs. This arouses an interest in reinforced retaining walls. This paper presents an example of the behaviour of reinforced retaining wall subjected to the subsoil deformation. One of the earliest analyses of the influence of subsoil deformation on structures was carried out by WASILKOWSKY [4]. The methods applied in structural analysis were based on a flexible range of work for subsoil and structure. Then the analysis was expanded in such a way as to include elastoplastic and viscoplastic models, see, e.g., KWIATEK [3], MAJEWSKI [2] and FLORKOWSKA [1].

The paper presents the results of computations concerning the analysis of reinforced retaining wall subjected to subsoil deformation. The problem was solved using two types of models: the Drucker–Prager model and the Cap model. The results given by these two models were compared.

2. ANALYSIS AND RANGE OF THE TASK

In this paper, a reinforced retaining wall presented in figure 1 was analyzed. In the structure of interest, five different material zones were separated: subsoil, embankment, reinforcement in the ground, contact surface and wall face. Calculations were carried out for two models of ground.

The analysis of the type of model was conducted based on the behavior of embankment. In order to build geometrical model, we used quadrilateral finite elements

method for incompressible media that are subjected to loosening. Then these media were implemented in Z-Soil system [5].

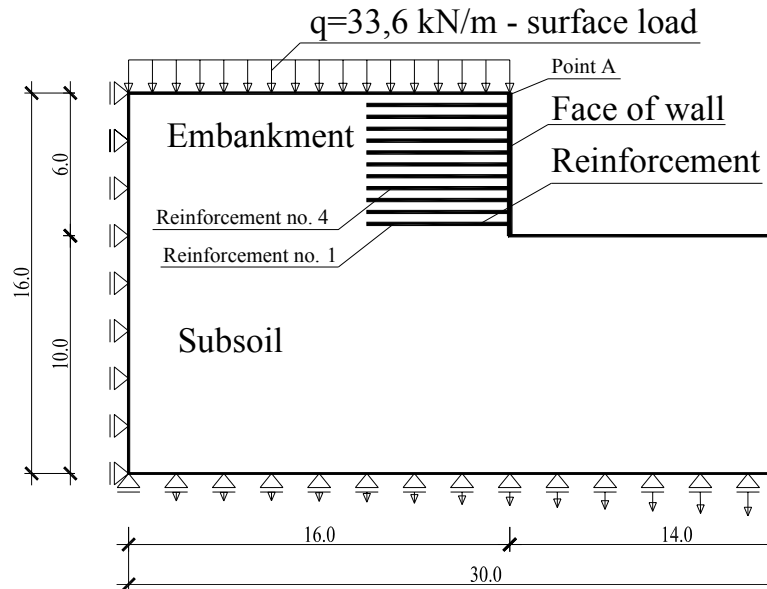


Fig. 1. Geometry of the model assumed for numerical computation

Deformations of the system analyzed were connected with the self-weight of back-fill ground while constructing the wall, and later on with the service load applied in the surcharge as well as with mining deformations acting in the direction perpendicular to the wall and the embankment axis.

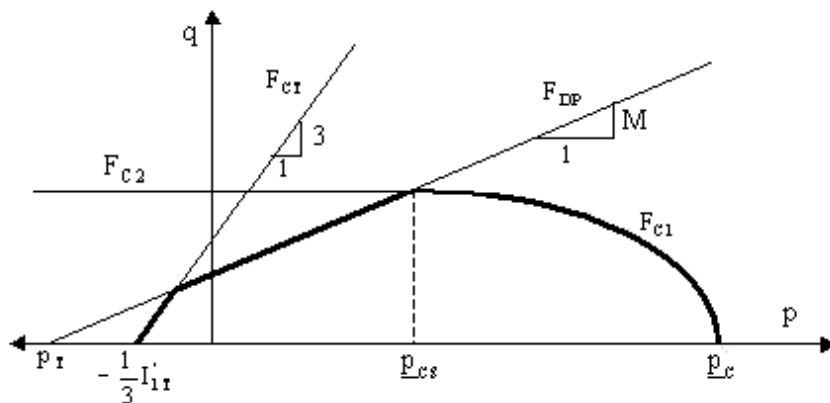


Fig. 2. Yield surface in the model assumed for the numerical computation

Based on the Drucker–Prager elastoplastic yield criterion we assumed that the material in the subsoil zone was isotropic. In the other case, the Cap model was added. Elastic properties of material were characterized by the modulus of elasticity E and Poisson's ratio ν , while plastic properties by the cohesion c and internal friction angle ϕ . For the other model the following parameters should be additionally assumed: the cap shape parameter R , the initial preconsolidation pressure P_{co} and the compression index λ .

Assuming associated flow rule in the plain state of strains we can present the yield surface in the Drucker–Prager model (figure 2) in the form:

$$F_{DP} = a_\phi \cdot I_1 + \sqrt{J_2} - k = 0. \quad (1)$$

For the Cap model we accept additionally:

$$F_{C1} = q^2 + \frac{M^2}{(R-1)^2} \cdot (\underline{p} - \underline{p}_c) \cdot (\underline{p} + \underline{p}_c - 2\underline{p}_{cs}) = 0, \quad \underline{p} \geq \underline{p}_{cs}, \quad (2)$$

$$F_{C2} = q^2 + \frac{M^2}{(R-1)^2} \cdot (\underline{p}_{cs} - \underline{p}_c) \cdot (\underline{p}_c - \underline{p}_{cs}) = 0, \quad \underline{p} < \underline{p}_{cs}, \quad (3)$$

where:

I_1 – the first invariant of stress tensor,

J_2 – the second deviatoric stress invariant,

a_ϕ, k – material constants as the function of c and ϕ from Coulomb–Mohr's model.

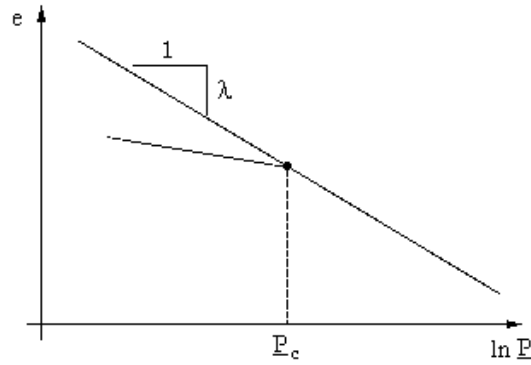


Fig. 3. Graphic interpretation of the parameter λ describing the slope of the e versus $\ln P_c$.

Loads acting within the subsoil medium are as follows: the self-weight γ , the stresses induced by external loads connected with the structure exploitation in the area of mining damage.

The shift of the mining trough is characterized by five parameters: subsidence, inclination, curvature, horizontal displacement and strain. Terrain curvature and hori-

zontal strain directly evoke additional loads in structures. The shift of trough may be divided into two phases. In the first phase, we deal with a convex terrain curvature with tensile horizontal strains, while in the second phase – with a concave curvature with compressive horizontal strains. Subsoil displacements being a result of mining exploration were assumed on the basis of the Budryk–Knothe theory [3].

The shift at the edge of the geometrical model was assumed to be adequate to the third category of mining damage according to appropriate Polish Code. Parameters taken for the analysis correspond to the following conditions: the radius of influence $r = 137$ m and the maximum subsidence $w = 1.37$ m. Calculations were done by analyzing the behaviour of the whole system (structure and subsoil) with two types of model ground.

3. SOLUTION OF THE PROBLEM

The problem was solved by means of finite element method. For the analysis conducted the discrete model for the area was applied. Half of the whole area was selected for analysis taking advantage of the symmetry of the system. The whole model consisted of 3096 quadrilateral finite elements, 288 beam elements modelling reinforcement and 522 contact elements describing the contact between subsoil and reinforcement as well as the wall face (figure 4).

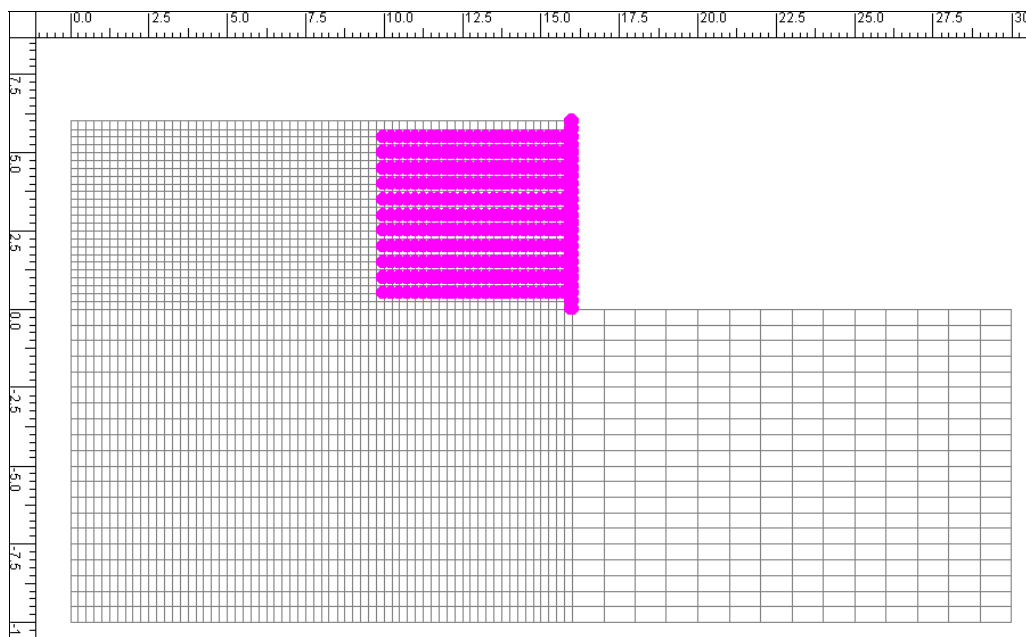


Fig. 4. Nodal network of the model analysed

It is assumed that the area being weightless at the beginning is gradually loaded with the self-weight. Within the next embankment with reinforcement, wall face is constructed stage by stage (steps 0–8). Then the external service load, corresponding to A class road, is applied to the embankment surcharge (steps 8–9). Finally (steps 9–13), there was analyzed the influence of shift of trough by means of horizontal and vertical strains equal to 6‰ and curvature of trough being 9000 m.

The values of the parameters for each material zone are as follows:

1. Subsoil: $E = 15.0$ MPa, $\nu = 0.3$, $\gamma = 20.0$ kN/m³, $c = 21$ kPa, $\phi = 13^\circ$, $\lambda = 0.15$, $P_{co} = 169$, $R = 1.29$.
2. Backfill: $E = 40$ MPa, $\nu = 0.3$, $\gamma = 17.5$ kN/m³, $c = 1$ kPa, $\phi = 13^\circ$, $\lambda = 0.15$, $P_{co} = 210$, $R = 1.30$.
3. Reinforcement of the soil:
Spacing between geogrid layer is 0.5 m, and weight is 1.24 kg/m².
Force due to 2% strain equals 52.5 kN/m.
4. Contact elements: friction angle between backfill and reinforcement: $\phi = 30^\circ$.
5. Face of reinforced soil: concrete: $E = 27$ GPa, $\nu = 0.2$, $\gamma = 25$ kN/m³, thickness of the face – 0.08 m.

4. RESULTS OF THE NUMERICAL ANALYSIS

4.1. RESULTS OF THE NUMERICAL ANALYSIS FOR THE VALUES OF FORCES IN THE REINFORCEMENT

In order to present the influence of mining deformation on the structure made of reinforced soil, the values of forces in selected reinforcement layers are given. These values were presented for two layers no. 1, 4. (figure 1). The diagrams presented show a general behaviour of the respective reinforcement layers.

The biggest influence of the model taken to the analysis of deformation on the structure of reinforced soil is visible in the first layer of reinforcement (figure 5). The forces in the first layer are twice as big as these in the second layer.

During the simulation of constructing the reinforced retaining wall and loading it with the forces from the traffic there is no difference in the values of forces, depending on the model chosen for calculations. The difference in the values of forces is seen very clearly beginning with the step no. 9. and becomes clear beginning with the step no. 10. The values of forces for the Drucker–Prager model are bigger during the deformation process. At the end the difference is equal to 6.0 kN/m.

In order to present the forces in consecutive layers of the reinforcement, layer no. 4 was chosen (figure 6). In the layers no. 2–6, the changes in the values of forces during the deformation process are analogous to those presented in figure 5. It can be seen that in the first stage, there is no difference in the values of forces (until step no. 9 is reached). Next, contrary to the layer no. 1, the bigger values are observed in the Cap model. It is especially visible at the end of deformation process. The difference in values is equal to 1.3 kN/m.

In the case of the remaining layers, no visible differences in the values of forces, depending on the given model, were observed. The shape of the diagram is analogous to that of the previous diagram.

4.2. RESULTS OF THE NUMERICAL ANALYSIS OF DISPLACEMENTS

Figures 7 and 8 present the diagrams of horizontal and vertical displacements during the deformation of the subsoil in the chosen point *A* (figure 1).

In the case of horizontal displacements (figure 7) their increase is observed during the tensile phase (steps 9–10), and in later phases the displacement increases insignificantly until step no. 12 is reached, and then it comes back to the maximal value. Beginning with the step no. 9 there is a difference in the values of horizontal displacements, depending on the model chosen. During the process of subsoil deformation the values of displacements in the Cap model are smaller than those in the Drucker–Prager model. The maximal difference is equal to 5.0 cm.

In the last phase of deformation (steps 12–13), the values of horizontal displacements in the Cap model are bigger than these in the Drucker–Prager model, but the difference is not significant as it is equal to 1.3 cm.

Vertical displacements (figure 8) after the trough shifting do not return to their initial values. The difference in the values of vertical displacements, depending on the model chosen, are visible beginning with the step no. 8.

In the Drucker–Prager model, the displacement values increase from step no. 8 to step no. 10, then their values remain on the level similar to that in step no. 12, and next they increase to the maximal value. In the case of the Cap model, a significant increase in the values of displacement is visible during the loading of the embankment surcharge with the traffic (steps 8–9). Afterwards the values of displacement increase until step no. 10 is reached. Between steps no. 10 and no. 12 a difference in a qualitative behaviour of the displacements can be observed.

5. CONCLUSION

Based on the numerical analysis conducted for the structure considered the following conclusions may be drawn:

Comparison of the values of forces in the reinforcement calculated on the basis of the Drucker–Prager model and Cop model reveals that the biggest difference is visible in reinforcement no. 1 situated at the bottom of the reinforced retaining wall. In the other layers of reinforcement, the differences are not so significant as in the layer no. 1.

In the case of horizontal displacements, there are no significant differences in values after completion of deformation. They are visible during the process of deformation, between steps no. 9 and no 12. In the Drucker–Prager model, horizontal displacements are stable with a slight tendency to change, whereas in the case of the Cap model there is observed a constant increase in the values of displacement, which lasts until the end of deformation. The biggest differences are observed in the case of the values of vertical displacements. Final value of vertical displacement in the Cap model is twice as big as in the Drucker–Prager model.

REFERENCES

- [1] FLORKOWSKA L., WALASZCZYK J., *Numeryczne modelowanie współpracy budynków z górotworem*, Materiały konferencyjne XXV ZSMG, Zakopane, 2002.
- [2] MAJEWSKI S., *Sprężysto-plastyczny model współpracującego układu budynek–podłoże poddanego wpływom górniczych deformacji terenu*, Zeszyty Naukowe Politechniki Śląskiej, seria Budownictwo, z. 79, nr 1271, Gliwice, 1995.
- [3] *Ochrona obiektów budowlanych na terenach górniczych*, praca zbiorowa, Wydawnictwo GIG, Katowice, 1997.
- [4] WASILKOWSKI F., *Pełne zabezpieczenie budowli przed szkodami górniczymi*, Inżynieria i Budownictwo, nr 7–8/51, 4/52, 3/53, 2/55.
- [5] Z_Soil v. 4.2, *Soil and rock mechanics on microcomputers using plasticity theory*.